RESEARCH ARTICLE

Norman Kerle · Benjamin van Wyk de Vries ·
Clive Oppenheimer

New insight into the factors leading to the 1998 flank collapse and lahar disaster at Casita volcano, Nicaragua

Abstract During unusually high rainfall associated with Hurricane Mitch in 1998, a flank collapse leading to a disastrous lahar occurred at Casita volcano, Nicaragua. The lack of a similar failure during a rainfall event of comparable magnitude in 1982 (Tropical Storm Alleta) suggests that additional factors influenced the 1998 collapse. We have investigated the potential contribution of erosional flank undercutting, seismic activity and anthropogenic land-cover change at the collapse site. Except for seismic events prior to Mitch, which may have increased flank instability, none of these factors appears significant. Instead, for failure to occur, the following conditions were required: (1) highly fractured slope material allowing deep and rapid infiltration of meteoric water, (2) a less permeable underlying layer to obstruct drainage, (3) strong, continuous antecedent rainfall to build up high pore-water pressure, and (4) episodic, high-intensity precipitation during Mitch to generate recurrent pressure waves. Prerequisite (1) was provided by edifice-wide deformation towards the south-east, seismic activity and proximity to a prominent fault, and local subsidence. Condition (2) was met by clay-rich layers resulting from hydrothermal alteration. More than 1,900 mm of rain fell in the 6 months prior to Mitch without significant interruption, while intense episodic precipitation occurred during the hurricane, satisfying conditions (3) and (4), respectively. The main difference with Alleta was that it occurred at the beginning of the rainy season and,

therefore, without sufficient antecedent rainfall. Anthropogenic activity, including land-cover change, did not affect slope stability (i.e. the hazard). However, vulnerability was generated when two towns were established in the lowlands south of Casita, on top of previous lahar deposits. It was greatly increased when approximately 4 km of forest between the collapse site and the towns were cleared, paving the way for a largely unobstructed debris flow. Deforestation also facilitated erosion along the flanks to provide about 78% of the material contained in the lahar when it destroyed the towns, killing more than 2,500 people.

Keywords Flank collapse · Gravity slide · Hurricane Mitch · Lahar · Nicaragua

N. Kerle (✉) · C. Oppenheimer
Dept. of Geography, Volcano Remote Sensing Group,
University of Cambridge,
Cambridge, CB2 3EN, UK
e-mail: kerle@itc.nl

B. van Wyk de Vries
Magmas et Volcans (UMR 6524),
OPGC Université,
Blaise Pascal, Clermont-Ferrand, France

Present address:
N. Kerle, ITC, Enschede, The Netherlands

Introduction

Structural instability in active and inactive volcanoes is a well-documented phenomenon (McGuire 1996). Processes leading to loss of structural integrity are varied and occur on a range of timescales, from short-lived eruptive activity, to gravitational settling over millennia (Dieterich 1988; Borgia et al. 2000). Different processes can also occur simultaneously. A variety of triggers, as diverse as dyke intrusion, earthquakes and rainfall, translate instability into active failure comprising anything from shallow surface layers to significant portions of the edifice (sector collapse).

More than 2,500 lives were lost when a flank collapse led to a lahar that descended Casita volcano in October 1998 and destroyed two towns (Fig. 1). The event was immediately attributed to strong rainfall produced by Hurricane Mitch, which was devastating large parts of Nicaragua and Honduras at the time. The initial belief in a breached crater (releasing ponded rain water) as the source of the disaster was quickly discredited (Sheridan et al. 1999). A post-disaster structural study, based on image analysis and analogue modelling, identified edifice-wide deformation at Casita, with a gravity slide forming in the
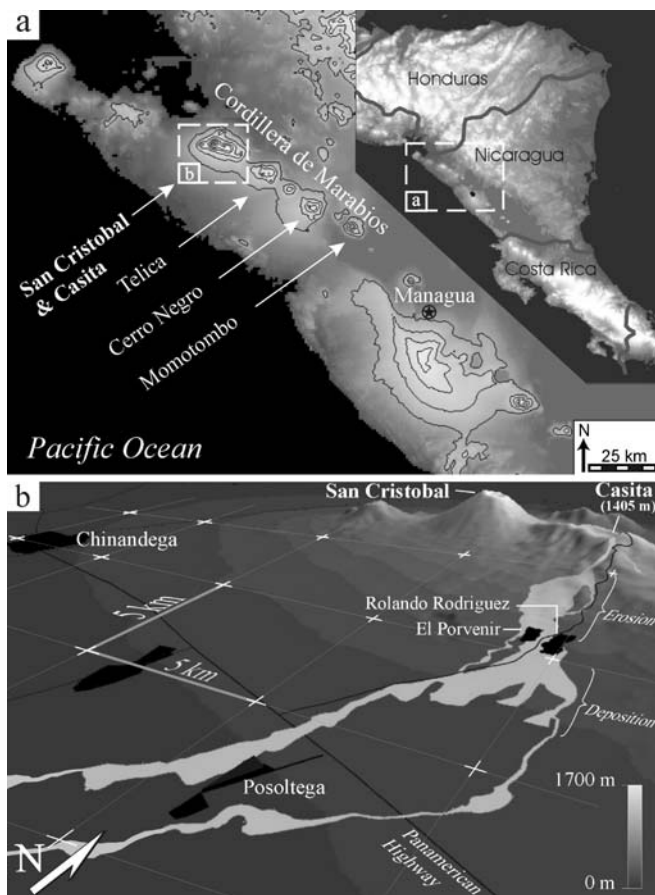
Fig. 1 a Map of Casita volcano within the Cordillera de Marabios. **b** Illustration of the extent of the 1998 debris avalanche and lahar event. The flow destroyed the towns of El Porvenir and Rolando Rodriguez (>2,500 fatalities), several bridges along the Panamerican highway and led to further fatalities in Posoltega. Rainfall data during Hurricane Mitch were collected at the Chinandega weather station, located approximately 20 km west and 1,300 m below the Casita summit

trigger, and (3) land-cover change in the vicinity of the failure area. Prominent gullies downslope from the failed flank were also surveyed with a Geodimeter Total Station before and after the 2000 rainy season (April to November), to assess the rate of erosion-induced morphological changes of gullies denuded by the avalanche. Lastly, uncertainty remains about the true rainfall amount at Casita during the hurricane, as published figures correspond to data collected at the Chinandega weather station, some 20 km west of and more than 1,300 m lower than Casita (1,405 m a.m.s.l.; Fig. 1b). New data sources, as well as simultaneous data collection at Chinandega and Casita during the 2000 rainy season, provide insight into Casita's orographic effect and the actual precipitation in October 1998.

Geological setting

Casita is part of the San Cristobal volcanic complex, located within the Cordillera de Marabios (Fig. 1). In contrast to the active San Cristobal stratocone, Casita constitutes a deeply dissected cratered ridge resulting from prehistoric W–E migration of activity. The volcanic complex is predominantly made up of island-arc tholeiite and calc-alkaline basalt (Hazlett 1987). Casita's summit, however, consists of autobrecciated dacitic domes, marked by extensive fumarolic fields (Sheridan et al. 1999). There is no evidence for historic eruptive activity at Casita, with final edifice construction probably ceasing about 8 ka ago (Scott et al. 2001).

The 1998 Casita lahar

Following the cessation of eruptive activity, persistent hydrothermal activity continued to weaken the edifice. Being buttressed by San Cristobal to the west, Casita began deforming in the opposite direction. Previous structural and morphological analysis, supported by analogue modelling, has identified plastic deformation towards the east, evidenced by convex–concave slopes, while a gravity slide of approximately 1.8 km in plan view and headwalls up to 100 m in height dominates the south-eastern sector (Fig. 2d; van Wyk de Vries et al. 2000; Kerle and van Wyk de Vries 2001). The lahar event began as a collapse along a relatively steep (average pre-failure slope angle of 35°), and approximately 400 m long section of this headwall, some 250 m south-west and 100 m below the summit. An estimated 1.6×10^6 m³ of flank material detached, leaving behind a steep scarp with slopes of 45–60° (Kerle 2002). The failure material, composed of hydrothermally altered and brecciated lava and tephra lithologies, disaggregated to form a debris avalanche that descended a ravine of 18° decline and 200 m width. Following deposition of its coarse bedload and a brief phase as a hyperconcentrated flow, the avalanche transformed into a mudflow that destroyed the towns of El Porvenir and Rolando Rodriguez, located

south-east sector (van Wyk de Vries et al. 2000). The morphology associated with the slide, consisting of steep and brittle slopes caused by deformation towards the south-east, was identified as the underlying reason for instability along the flank that subsequently failed, with Mitch only acting as the trigger (Kerle and van Wyk de Vries 2001).

However, the apparent causality between rainfall and flank collapse is put into question by archived meteorological data, which show a similar rainfall episode during Tropical Storm Alleta in 1982 (INETER 1999). No disastrous flank failures occurred during that event, and effects were limited to shallow debris flows that led to two fatalities (Morales 1998), raising the question of how the 1998 situation differed. The purpose of this study was to investigate whether additional processes that are known to compromise slope stability contributed to the 1998 Casita failure. We address (1) possible upslope gully propagation leading to undercutting of the failure flank, (2) recent seismic activity in the region or a seismic

Fig. 2 a Pre- and **b** post-disaster DEMs of Casita, surface-draped with corresponding aerial photographs acquired in 1996 and 2000. Note how edifice-wide deformation has resulted in a triangular gravity slide along Casita's southern flank, forming adjacent ravines through which avalanche material descended following the flank collapse (*solid lines* indicate failure scarp). The locations of gullies G1 and G2 surveyed before and after the 2000 rainy season are indicated. **c, d** 1996 stereogram of Casita's south-east sector, with major faults and deflected drainage channels indicated. All stereograms in this paper are best viewed with a standard pocket stereoscope
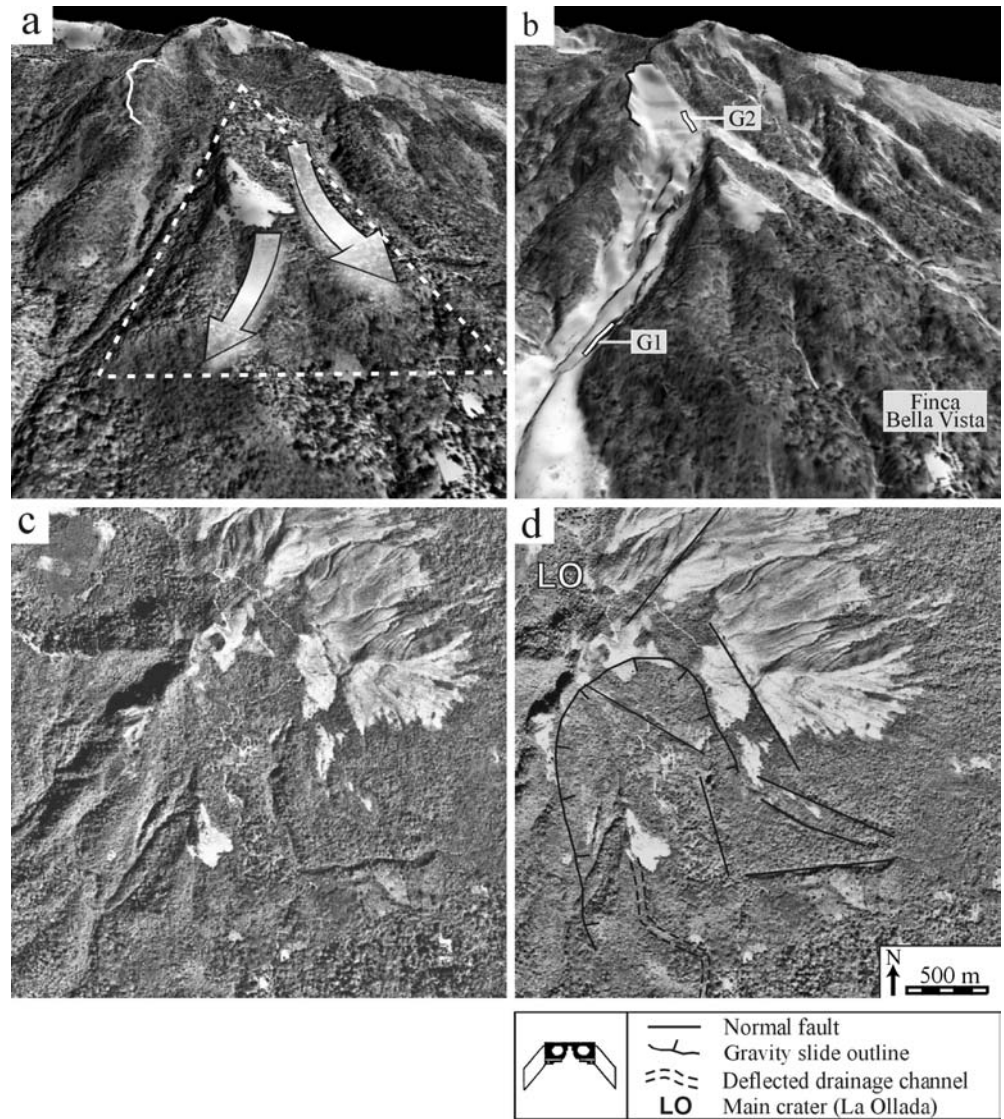
more than 6 km from the failure site (Scott et al. 2003). Significantly, less than 22% of the matrix-size lahar deposits (particle size <2 mm) originated from the initial failure material, the remainder having been entrained (bulked) following the widening of the flow upon leaving the ravine (Fig. 1b; Scott et al. 2003). Deposition increased downstream from the towns, in places reaching a thickness of up to 2 m. The deposits generally lack gradation, and are dominated by pebble-sized clasts suspended in a fine matrix, containing occasional boulders (Scott et al. 2003). The loss of solids caused the lahar to transform into a hyperconcentrated flow, which destroyed bridges along the Panamerican highway, led to damage and further fatalities in the town of Posoltega, and continued as a sediment-laden streamflow towards the Pacific Ocean.

In addition to crater-lake breach, the event was also blamed on magmatic activity (following reports of hot mud), and ground shaking caused by earthmoving equipment that had been used for road improvement in the summit area (Morales 1998). However, these allegations were subsequently discounted, and research over the 3 years following the event has uncovered no evidence for any of those outside trigger mechanisms. For a detailed description of the flow event see Kerle and van Wyk de Vries (2001); for a sedimentological study detailing evidence for the described flow transformations see Scott et al. (2003).

Temporal changes in gully morphology

Figure 2 shows pre- (a) and post-event (b) digital elevation models (DEMs) of Casita's south-eastern flank, surface-draped with aerial photos taken in 1996 and 2000, respectively. The DEMs outline the crescentic gravity slide that is marked by steep headwalls, which enclose a roughly triangular area delimited in the east and west by prominent ravines, and by basal thrusts in the south. The main debris avalanche followed the western one of the

ravines, while approximately 15% of the material overflowed into the eastern ravine (Scott et al. 2003). An analysis of the structural features, including the steep, horseshoe-shaped rim, and deflected fault lines and drainage channels (Fig. 2c, d) has suggested ongoing edifice deformation (Kerle and van Wyk de Vries 2001), which is thought to have begun at least 500 years ago, and is considered to be the result of a hydrothermally altered core (van Wyk de Vries et al. 2000). Such deformation, however, also implies the possibility of changes in erosion patterns, and an active headward propagation of gullies located within the western ravine originating at the collapse site (Montgomery and Dietrich 1988, 1989; Hovius et al. 1998). A set of aerial photos spanning 42 years (Table 1) was obtained to investigate such temporal changes in gully size and extent. Three stereo, pre-event datasets, acquired in 1954, 1987 and 1996, were used in the analysis. While an orthorectification of the 1996 photos was possible, poor image quality and lack of camera information for the 1954 and 1987 photos precluded using them for topographic correction. However, image quality and scale were sufficient for all datasets to be used in a qualitative stereoscopic analysis in ERDAS Imagine's StereoAnalyst (essentially a digital stereoscope). Figure 3 depicts stereograms of the Casita failure area and the western ravine, which is dominated by two principal gullies. Each stereo-pair is complemented by a drawing that outlines areas of hydrothermal alteration, the principal and secondary gullies and depressions, and the extent of the flank failure. Note that the stereograms are vertically exaggerated as a function of photo-overlap and flying height, which must be considered during photo interpretation. When viewed with a pocket stereoscope, it is apparent that the overall shape of the gullies in 1996 was not different from 1954 and 1987. An apparent decline in hydrothermal activity over the time period covered by the photos, associated with an increase in vegetation cover, is likely to have contributed to the stability. Only the shallow depression upslope from the principal gullies had grown in extent. Of greater concern for flank instability appears to be a depression labelled D1 in the 1954 structural map. However, the apparent undercutting of the slope is virtually unchanged in the 1996 photos.

The stabilising effect of vegetation was lost when the avalanche denuded the ravine (see Mejia-Navarro et al. 1994). To test for short-term changes in morphology, two gullies, G1 and G2 (Fig. 4a and b, respectively, locations marked in Fig. 2b), were surveyed. The surveys were carried out in March and November 2000, effectively bracketing the annual rainy season. Approximately 1,600 mm of precipitation were recorded in Chinandega during that time, including more than 400 mm between 30 September and 3 October during Hurricane Keith (INETER, archived data). For each gully, between 170 and 350 measurements were collected with a Geodimeter Total Station during each survey, resulting in detailed DEMs with 0.3-m grid spacing. Figure 4c, d illustrates the topography of both channels before the rainy season. The

lack of significant long-term change in gully morphology observed during the time-series photo interpretation was mirrored by the survey. Despite strong rainfall and lack of vegetation, no appreciable changes occurred along the gully heads. Figure 4e, f shows superimposed contours for both gullies, interpolated from the respective pre- and post-rainy season data. Profiles for the actual gully head (thick hatched line, and solid white line in c, d) are virtually unchanged. The survey suggests that gradual erosion from surface runoff plays a limited short-term role in gully propagation. This can be explained by the slope material, which consists of block- and boulder-rich deposits from previous avalanches, which provide resistance to fluvial erosion (Fig. 4a, b; see also Fig. 5 in Kerle and van Wyk de Vries 2001). Previous studies, both in temperate (Montgomery and Dietrich 1988; Dietrich et al. 1993) and tropical (Hovius et al. 1998) environments, have identified mass failures along gully heads as the primary engine for drainage network expansion. The lack of steady, erosion-induced morphological change in the surveyed gullies, even under favourable conditions, points to a similar mechanism at Casita.

While the morphology of the western ravine shows high temporal stability, significant changes occurred near the top of the failure scarp (indicated by the solid black line in Fig. 3). The north-eastern section of the hydrothermal field contains an oval-shaped depression (D2 in Fig. 3a). In 1954 it was only faintly apparent, and had a length of approximately 60 m. By 1996 it had deepened and extended to about 110 m in length, as illustrated in the close-up stereograms shown in Fig. 5b, c. By the time of failure, the section had extended along more than a quarter of the length of the eventual failure scarp, and was entirely incorporated in the collapse material (Fig. 3c). Although the magnitude of the change in depth can not be quantified due to the aforementioned inferior quality of the 1954 photos and lack of camera information, the increase in size in all three dimensions is clear. The depression further corresponds precisely to an area of highly fractured and brecciated lava and tephra, strongly hydrothermally altered, and with clear signs of subsidence (Fig. 5a). The area is distinctly separated from a well-layered, largely undeformed and unaltered section to the south. This deformation would have fuelled further fracturing, and facilitated infiltration of meteoric water, the effects of which are discussed in more detail in a later section.

Regional seismic activity

Nicaragua is located in one of the most seismically active regions in the world, a result of the Cocos plate subducting beneath the Caribbean plate along the Middle America Trench (Fig. 6). This has given rise to the country's chain of volcanoes, including the Cordillera de Marabios, as well as to frequent earthquakes (Figs. 1a and 6). Nicaragua's capital, Managua, was heavily damaged by seismic events in 1885, 1931 and 1972.

Fig. 3a–c Stereogram time series of the 1998 flank failure site and the western ravine through which the initial avalanche travelled, and corresponding structural drawings. Photographs shown were acquired in **a** 1954, **b** 1987 and **c** 1996. The photos document a lack of significant morphological change in the principal gullies, an increase in depth and extent of a small depression (*D2*) within the failure area, and a decrease in hydrothermal activity, evidenced by increased vegetation cover
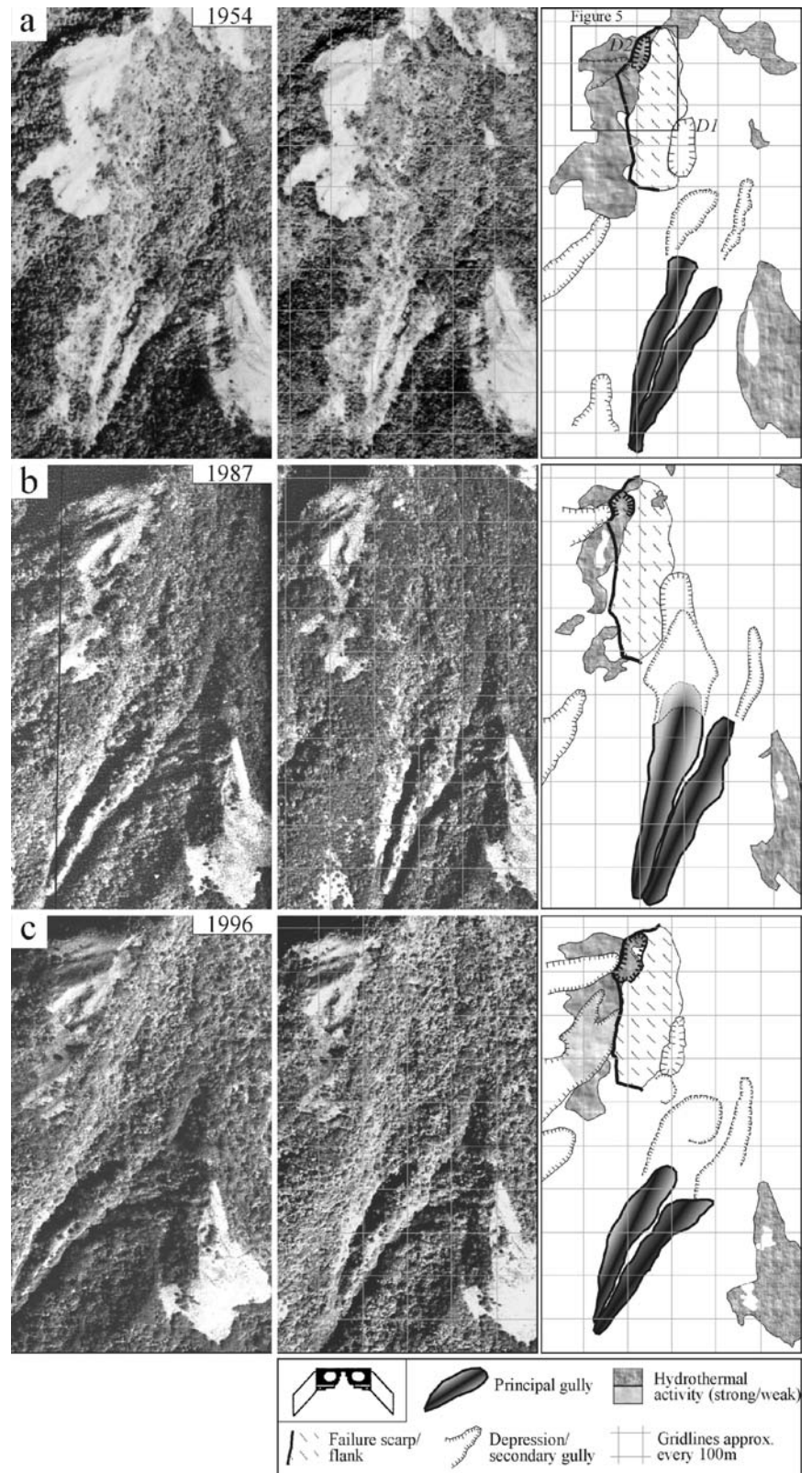
Casita's base is cut by tectonic faults striking at N30°W and N35°E (van Wyk de Vries and Merle 1998), as well as sub-radial volcanic faults around the summit (van Wyk de Vries et al. 2000). The most severe faulting is associated with the gravity slide, whose back wall is up to 100 m high and forms a crescent-shaped scarp, along which the 1998 failure occurred. Several other faults exist along the crescent and within the gravity slide (Fig. 2d).

Fig. 4a–f Analysis of morpho-
logical changes in two gullies
within the western ravine over
the course of the 2000 rainy
season. **a, b** Photographs of the
gullies, with the approximate
extent of the area surveyed (*thin
white line*) and the thalwegs
indicated. **c, d** DEMs of the
surveyed gullies, interpolated
from the pre-rainy season data
collected with a Geodimeter
Total Station. **e** Contour lines
calculated from the pre- and
post-rainy season datasets of
gully 1 and **f** gully 2 (refer to
Fig. 2b for gully locations).
Insets show elevation profiles of
the two gully heads, which
demonstrate that no upslope
gully propagation occurred
during the 2000 rainy season.
The profiles are marked by
solid white lines in **c** and **d**, and
*thick hatched lines* in **e** and **f**.
See text for discussion
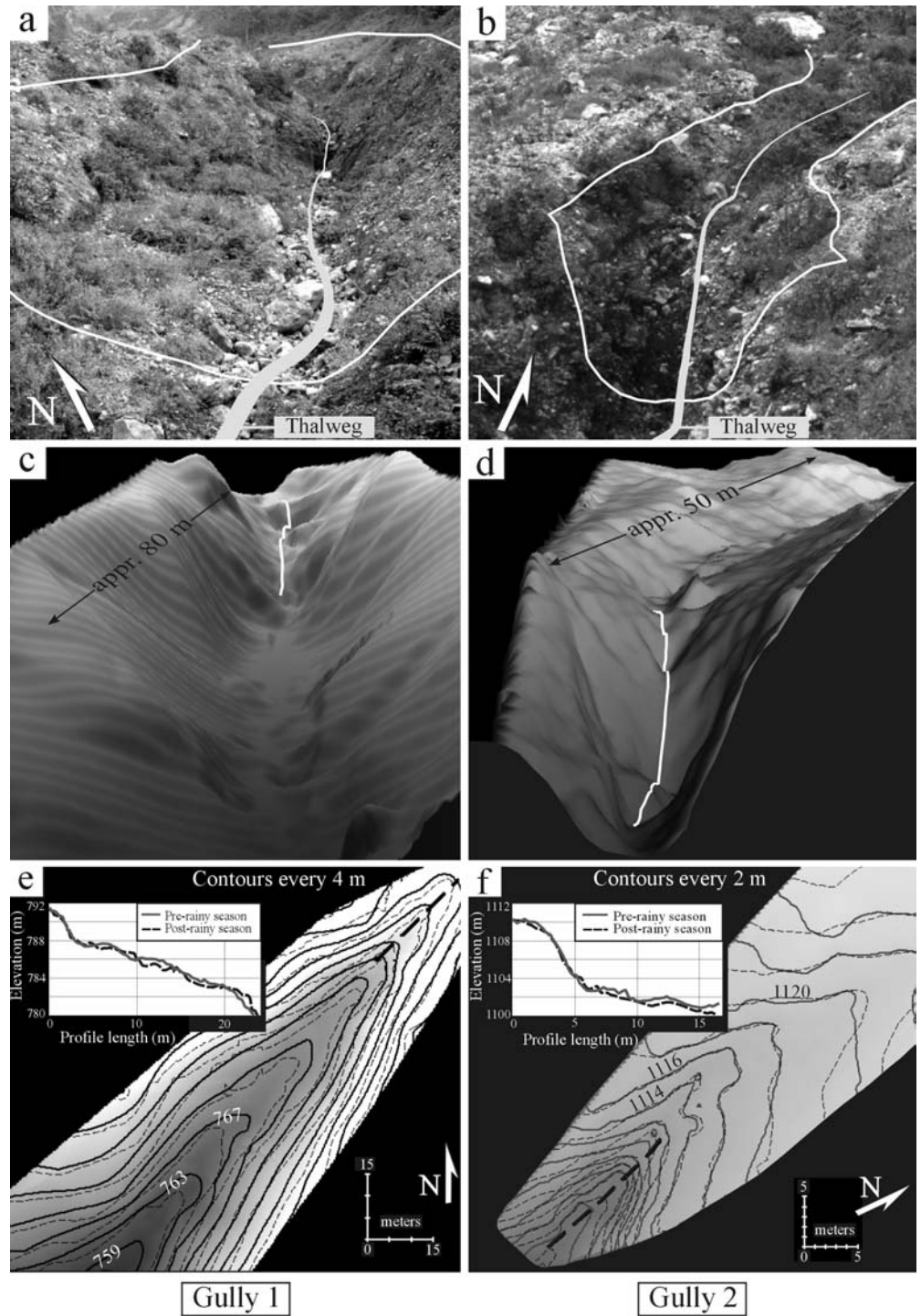
Table 1 Aerial photos used to
investigate temporal changes in
gully size and extent

Date of acquisition	Photo scale	Dataset used	Pre- or post-event	Mono or stereo
2 February 1954	1:30,000	X	Pre	Stereo
? 1970	1:17,500		Pre	Mono
5 December 1987	1:25,000	X	Pre	Stereo
14 January 1996	1:40,000	X	Pre	Stereo
4 December 1998	1:65,000		Post	Mono
4 January 2000	1:40,000		Post	Stereo
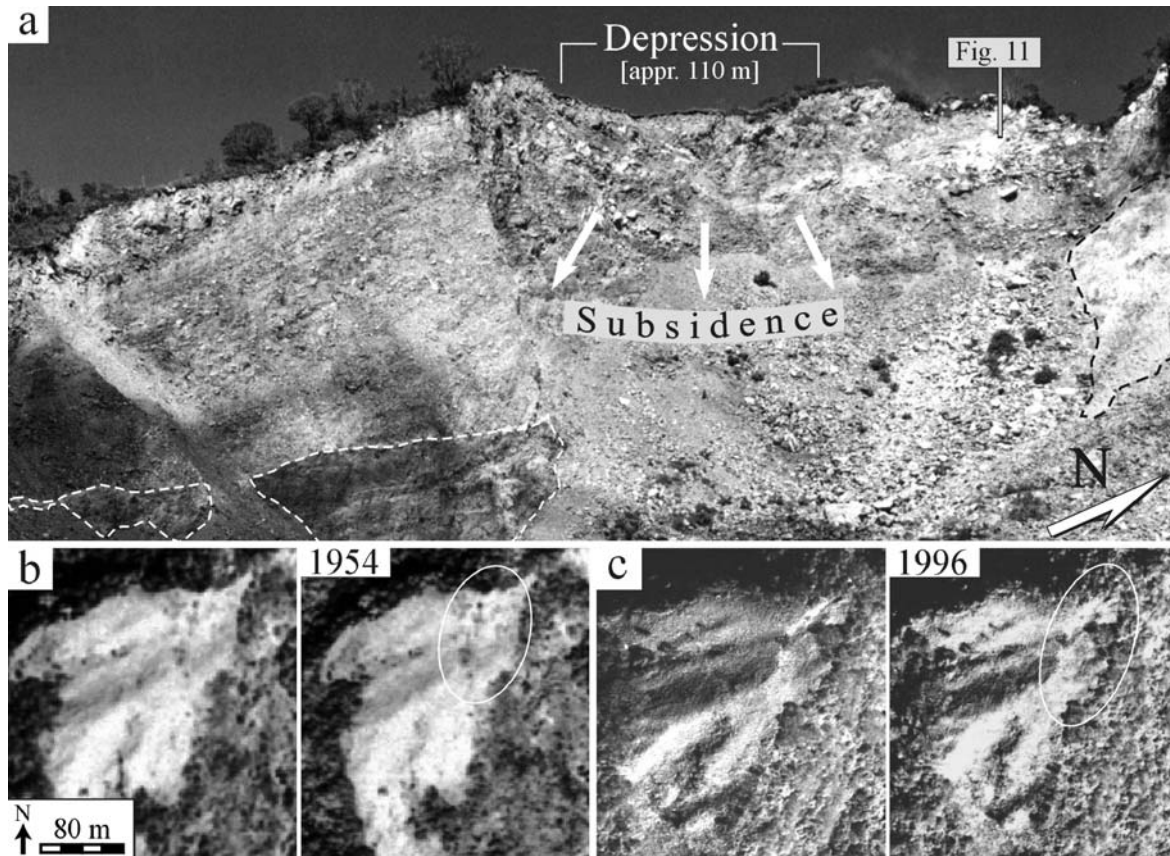
Fig. 5 a Photograph of the 1998 failure scarp, showing a central area of subsidence, marked by heavily hydrothermally altered and brecciated material. This area corresponds to the depression identified in Figs. 3a–c. **b, c** Large-scale stereograms of the depression, showing how the area has become larger and deeper between 1954 and 1996
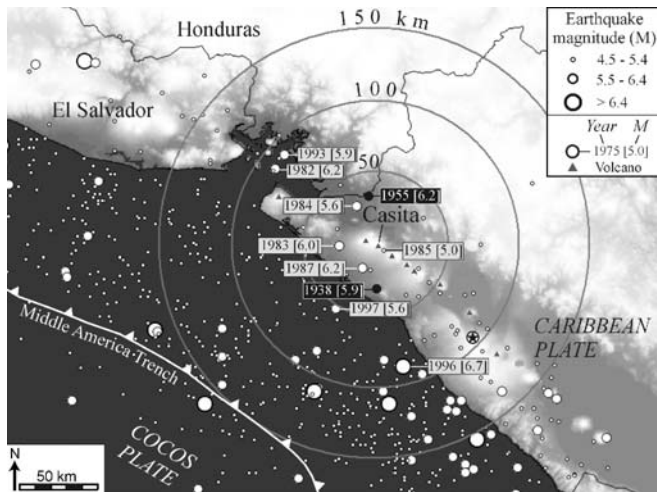
Fig. 6 Seismic events (magnitude ≥4.5) around north-west Nicaragua between 1982 and 1996. Earthquakes, as well as the volcanic chain indicated, result from subduction of the Cocos beneath the Caribbean Plate at the Middle America Trench. Several moderate to strong earthquakes had their epicentres in the vicinity of Casita volcano

See Kerle and van Wyk de Vries (2001) for a detailed structural map.

Seismic events with magnitudes of 4.5 or higher, which affected north-western Nicaragua between 1982 (post-Alleta) and 1996 (pre-Mitch) are plotted in Fig. 6. Several of those events occurred close to Casita, including a 5.0 event in 1985 with an epicentre only 8 km away (USGS, National Earthquake Information Centre). Much of this time period coincides with the Sandinista revolution and Contra war in Nicaragua, which only ended in 1990, and resulted in limited scientific data and reports of damage caused by natural events. No seismic data were archived by the responsible national research institute (Instituto Nicaragüense de Estudios Territoriales; INETER) between 1982 and 1993, and, to our knowledge, no reports of earthquake-induced damage in the Casita area exist for this time. Additionally, the temporal resolution of the Casita photo-series is not sufficient to correlate consequences of seismic activity, such as shallow landslides, with recorded earthquakes, especially given the rapid revegetation observed following the 1998 lahar.

Topographic rises, such as ridges and hilltops, are known to amplify seismic signals (Bouchon 1973; Geli et al. 1988). Spudich et al. (1996) documented a factor of ten

increase of seismic wave amplitude in a hill rising only 60 m above the surrounding plains during an earthquake in California. This effect has also been documented at Casita. During a magnitude 5.9 earthquake in 1938 (epicentre approximately 30 km south of Casita, with recorded intensities of VII on the Modified Mercalli scale; Rojas et al. 1993; Fig. 6), the Bella Vista finca, an agro-estate on the southern slope, was severely damaged (Fig. 2b). Local residents also reported higher seismic intensities towards the summit, asserting that people were thrown "more than 1 metre" high into the air (La Prensa, 28 April 1938). "Objects thrown into the air" are considered evidence of intensity XII. Although calculations by Bolt and Hansen (1977) have shown that lower intensities may be sufficient, such shaking likely has effects on flank stability, especially since horizontal acceleration typically exceeds vertical acceleration (Bolt and Hansen 1977). Damage caused to Bella Vista during the 1938 event was repeated by a magnitude 6.2 earthquake in 1955 (epicentre approximately 35 km to the north; USGS, National Earthquake Information Centre), which was also reported to have opened cracks and fissures on the volcano (La Prensa, 21 April 1955). Sapper (1913a) had attributed similar fissures on San Cristobal to an 1898 earthquake.

Land-cover changes

Land cover in north-western Nicaragua underwent fundamental changes during the last century. Much of it took place at the expense of original forest cover, mainly dry tropical forest, which is now considered extinct in western Nicaragua (European Forest Institute 2000). Land clearing for cattle production began to incise what von Seebach (1892) and Sapper (1913b) described as the extensive forest plains of Chinandega. At the time of Sappers's visit, Casita's base and flank were still covered with dense deciduous forest, with open pine forest and shrubs dominating at elevations above 1,000 m (Sapper 1913b). Extensive cotton farming led to further large-scale deforestation between the 1940s and 1970s, before falling cotton prices resulted in the collapse of the industry. By that time, however, large cattle- and cotton-enterprises had begun to push farmers onto subsistence plots higher on the volcanic flanks of the Cordillera de Marabios. Coffee growing, which had already existed on Casita and San Cristobal during Sapper's time, became more widespread. Land use on the volcano's flanks was further intensified after the Sandinista Revolution in 1979 led to a socialist-inspired agrarian reform. Despite efforts to protect the volcanic cones of the Marabios chain by banning development and agricultural use above 300 m, anchored in a 1983 decree by the Institute for Natural Resources and the Environment (IRENA, later MARENA), land on the volcanic slopes was allocated to individuals and cooperatives. Villages such as Santa Narcisa and Pikín Guerreo, the latter located above 600 m (Fig. 7b), were established on Casita's south flank at that time (J. Incer Barquero, former director of MARENA, personal communication).

The slopes and lowlands south-west of all Marabios volcanoes have traditionally been preferred for agriculture (and, consequently, settlements), a result of higher soil fertility afforded by the trade wind's preferential distribution of volcanic pyroclastics. With much of the forest cover cleared in the lowlands south of Casita, further cooperative settlements, notably El Porvenir and Rolando Rodriguez, were founded in this sector in the mid-1970s (Barreto 1998).

The 1954 and 1996 aerial photos, as well as a declassified 1967 Corona satellite photograph, were used to document deforestation on Casita's southern lowlands during that time, in particular in the area affected by the 1998 lahar. Figure 8 shows the extent and location of all images. The actual photographs show that by 1954 much of the belt between the Panamerican highway and the volcanoes had already been deforested. The continuation of that trend, especially north of the destroyed towns, is mirrored in the time-series presented in Fig. 7a. The extent of forests in 1954 (white), 1967 (light grey) and 1996 (dark grey) are superimposed. The white and light grey areas essentially depict the land deforested by 1967 and 1996, respectively. The individual images, with the lahar boundary overlaid, are shown as Fig. 7b–d. By the time the lahar occurred, of the 6 km of forest that originally separated the town locations from the lahar source, less then 2 km remained.

As a result of inaccessibility and hydrothermal activity, the actual source area of the 1998 lahar had no history of land use. Similarly, no deforestation at the base of the failed flank is documented in the aerial photographs; indeed, forest density appears to have increased here (see Fig. 3a, c). Figure 2c–d also conveys the inaccessibility of the ravine through which the avalanche descended. No land use within the ravine has been documented, and none is evident in the aerial photographs.

Rainfall during Mitch

A tropical depression formed south of Jamaica on 21 October 1998. It quickly gained strength and by 25 October had turned into category 5 Hurricane Mitch (Saphir–Simpson scale), one of the strongest storms to affect Nicaragua in historic times (INETER 1999). Without actually entering Nicaragua, the storm crossed Honduras and moved slowly north into Guatemala and Mexico while gradually losing power.

There is no specific moment in time when Mitch began to influence precipitation at Casita. INETER (1999; p. 58) states that Nicaragua was affected by the storm from 22–31 October 1998, with the Chinandega weather station recording the highest accumulated rainfall in the country during that time, a total of 1,597 mm. Although Mitch only made landfall in northern Honduras on 29 October, rainfall in north-western Nicaragua began to increase on 27 October, the result of an intense low-level south-

Fig. 7a-d Summary of deforestation on Casita's southern slope and in the area covered by the 1998 avalanche and lahar. **a** Outline of forested areas in 1954 (*white*), 1967 (*light grey*), and 1996 (*dark grey*). **b–d** Aerial and satellite photographs documenting how much of the forest that separated the towns of El Porvenir and Rolando Rodriguez in 1954 had disappeared by 1996, greatly increasing the vulnerability of the towns to lahars. The extent of the lahar deposits is outlined, as are the locations of the destroyed towns
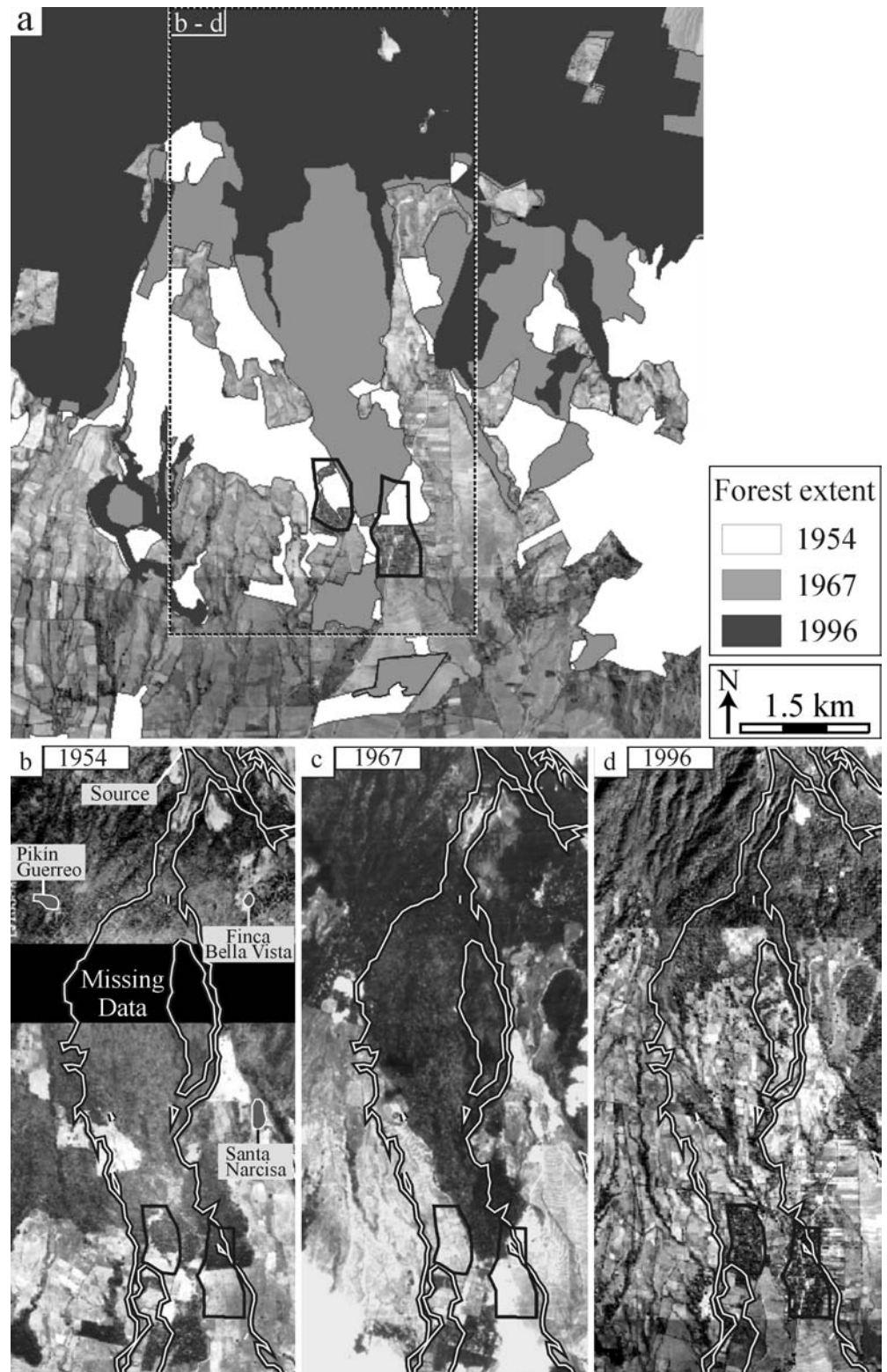
westerly flow spawned by Mitch's broad circulation (Ferraro et al. 1999; Fig. 9a). With the flank collapse occurring between 10:30 and 11:00 a.m. on 30 October, approximately 750 mm of rain were recorded over some 83 hurricane-affected hours before the disaster. The graph also provides an explanation for the slow official emergency response, and the disbelief in Managua meeting reports of the event at Casita (Kerle and Oppenheimer 2002) – rainfall in the capital was not abnormal. It also illustrates that precipitation in Chinan-
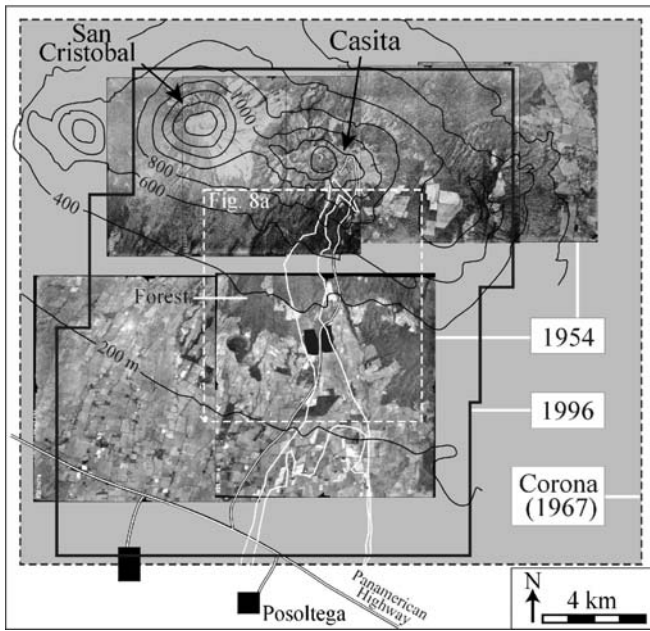
Fig. 8 Overview of images used in the assessment of land-cover change. The 1954 aerial photographs are shown, while the 1996 photos, and 1967 Corona satellite image are outlined in *solid* and *hatched lines*, respectively. Note that the 1954 photo set is of variable scale and incomplete, with a missing flight line resulting in a 1-km horizontal gap. The photos show, however, that extensive deforestation south of the Casita and San Cristobal volcanoes had already occurred by 1954

dega was episodic rather that continuous, with several high-intensity rainfall events per day.

Ferraro et al. (1999) suspected that Casita's orographic effect contributed to the high rainfall. No official rainfall measurements were carried out at Casita during the storm, as an existing rain gauge at the summit was not in use. However, precipitation data are collected for INETER by an employee of the Bella Vista finca. The values for the 2000 rainy season are similar to the Chinandega data (Fig. 9b), indicating a limited orographic effect of Casita's volcanic structure. However, during a visit to the finca in November 2000, records for that month were incomplete, suggesting that the data must be used with caution. Indeed, the values recorded at Bella Vista during Mitch are much lower than at Chinandega (Fig. 9b, inset), despite reports of many people from surrounding settlements seeking shelter from torrential rains in the towns that were subsequently destroyed (Scott et al. 2003).

In an attempt to calibrate the Chinandega data for any orographic effect, a weather station was deployed at Casita's summit in September 2000 (Fig. 9c). Despite one outlier and some temporal offsets, there is very good agreement between the Chinandega and Casita data for the 25-day observation period (257 vs 249 mm, respectively). Both outlier and offsets are likely artefacts of manual transcription of rain gauge data-strips, where sustained precipitation can be attributed either to the beginning- or the end-day of a rainfall event.
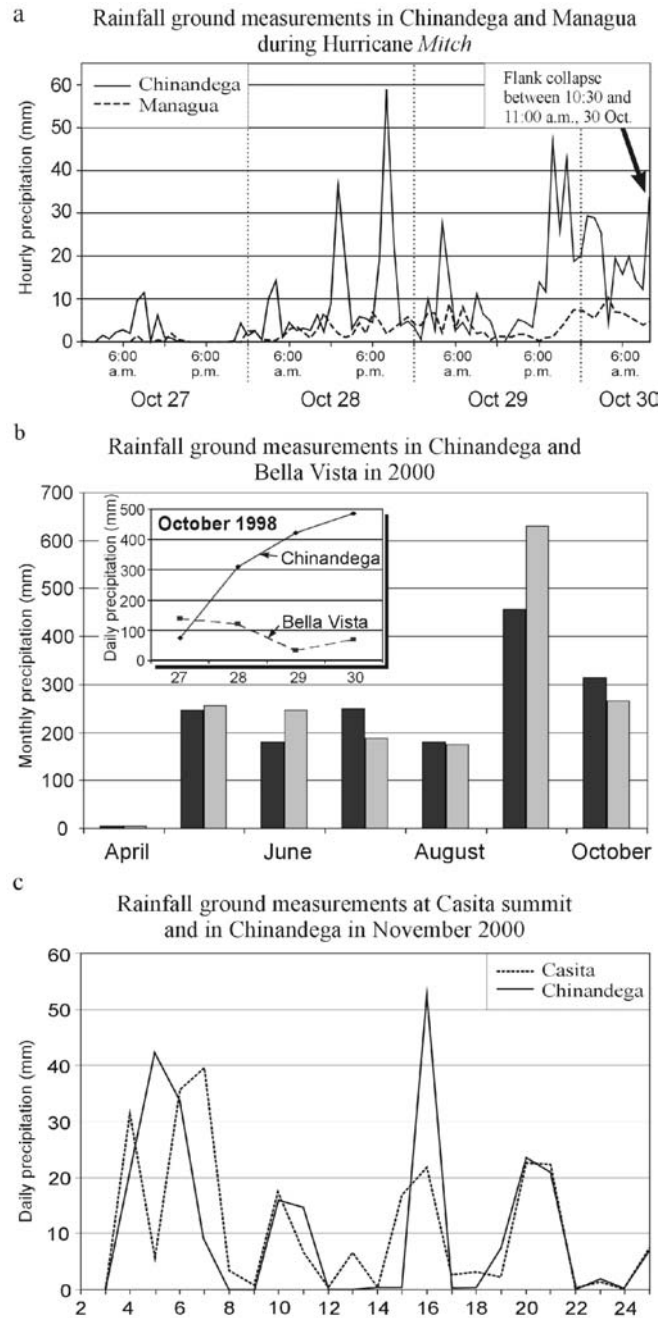
Fig. 9 a Hourly precipitation values recorded during Hurricane Mitch in Chinandega and Managua. For approximately 83 h before the collapse on 30 October, 1998, hurricane-related rainfall was recorded in Chinandega, while Managua was largely unaffected. **b** Monthly rainfall recorded in Chinandega and at Bella Vista (located above 700 m on Casita's south flank) during the 2000 rainy season. The data show good agreement, suggesting a limited orographic effect at Casita. However, daily values recorded at Bella Vista during Mitch are significantly lower than at Chinandega (for example 34 mm on 20 October, compared with more than 420 mm at Chinandega), casting doubt on their reliability (inset; source: INETER 1999). **c** Daily rainfall at Casita weather station and in Chinandega
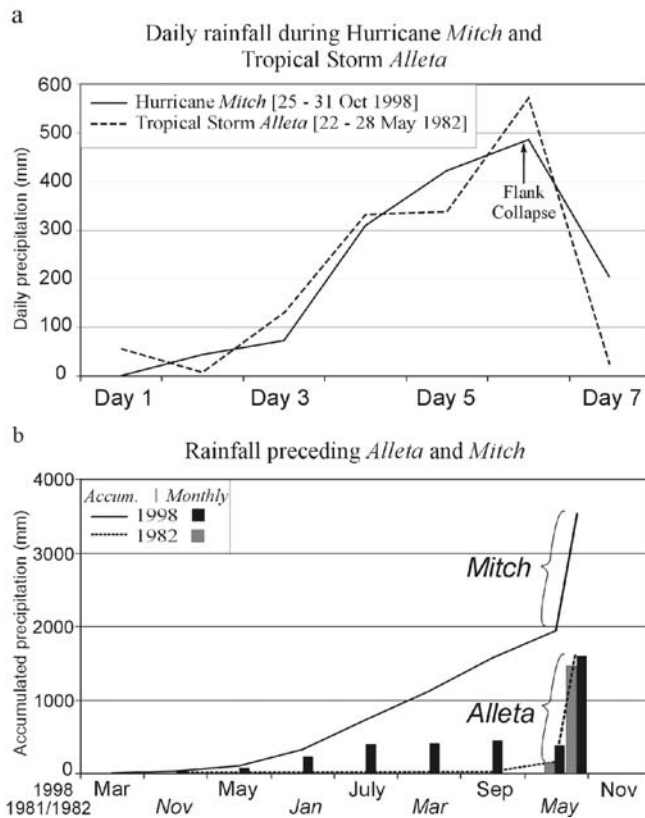
Fig. 10 a Normalised daily rainfall during Tropical Storm Alleta and Hurricane Mitch. Note that rainfall during both events was comparable (a total of 1457 vs 1,538 mm, respectively). b Accumulated rainfall in the months preceding Mitch and Alleta, plotted on a normalised, monthly scale. A total of 164 mm fell before Alleta, and more than 1,900 mm before Mitch (source: INETER 1999). Note the horizontal chronological offset in b for the 1981/1982 and 1998 data

Another approach to detect an orographic effect involved an analysis of rainfall data derived from half-hourly Geostationary Operational Environmental Satellite (GOES) data, provided by NOAA/NESDIS, using the Auto Estimator algorithm described by Ferraro et al. (1999) and Vicente et al. (1998). The satellite method provides instantaneous precipitation estimates, from which average hourly rates based on three consecutive images are derived. Although the values for Chinandega were lower than the corresponding ground measurements, there was no significant difference between the pixels corresponding to Chinandega and Casita. Given that the data collected in Bella Vista are potentially flawed, and the lack of evidence for an orographic effect, we apply the Chinandega value of 750 mm to Casita as well.

As noted earlier, tropical storm Alleta in 1982 did not lead to flank collapse, despite comparable rainfall (1,457 vs 1,538 mm over 7 days), and a higher daily maximum of 570 mm on 27 May 1982 compared with 485 mm on 30 October 1998 during Mitch (Fig. 10a; INETER 1999). The principal difference between the two events is the occurrence of Alleta at the beginning, and of Mitch at the

end of the rainy season. The accumulated rainfall plotted for both events in Fig. 10b shows that only 164 mm of rain were recorded at Chinandega over 6 months before Alleta, compared with more than 1,900 mm that fell in the 1998 rainy season prior to Mitch. Casita's infiltration capacity is well known, and is reflected in its indigenous name of Apastepe, meaning 'Hill full of water'. This refers to the absence of surface streams, and the abundance of wells in the lowlands at the foot of the volcano (J. Incer Barquero, personal communication). Infiltration rates as high as 119 mm in only 3 min were measured by one of us (NK) near the failure area. Given the watershed of the 1998 failure area of approximately 75,000 m^2, some 56,000 m^3 of rainwater would have fed into the failure material over the 83 h before the event. Together with significant previous precipitation, this resulted in infiltrated water accounting for at least 18% of the flank collapse volume (see Scott et al. 2003).

The effect of water on slope instability

Rock dissolution and precipitation of clay minerals during hydrothermal activity can reduce the cohesive strength and effective coefficient of friction in volcanic material, and lead to edifice weakness (López and Williams 1993). However, such processes do not necessarily result in collapse, as minerals also seal fractures, increasing the tensile strength of the rock. Stability is more effectively reduced by discrete faults, as well as pressure variation within fault and pore spaces (Day 1996). Pressure can be provided by a hydrothermal system (where venting is limited), dike intrusion (Elsworth and Voight 1996) or by infiltrating water. In particular deep-seated failures (depth >5 m) tend to be triggered by positive pore pressure caused by rising groundwater, whereby larger absolute amounts of water are needed with increased depth to offset the rising normal stress (van Asch et al. 1999). However, for failure to occur, high pore pressures must be established and maintained (Day 1996). Although heavy rainstorms temporarily raise the water table in well-jointed rocks, the same joints and cracks can also lead to rapid subsequent drainage. The pore pressures described by Day (1996) resulted from a low-permeability carapace capping the hydrothermal system. However, the same carapace also provides a barrier to infiltrating water. More than 1% of the Casita collapse material is thought to have been clay (K. Scott, personal communication), primarily accumulated in the area of subsidence, as well as in less-fractured, but highly altered bedrock (hatched lines in Fig. 5a). The exposed bedrock is sharply separated from overlying, well-layered pyroclastics, and likely continues further north, hidden by the scree slope seen in the photo. The extensive fracturing in the subsiding section, result-ing from the proximity to the gravity slide boundary fault that lies just below the failure cliff, subsidence itself, as well as seismic activity, provided the pathways for deep infiltration. It is possible, that a perched water table was created when the clay-rich bedrock impeded further
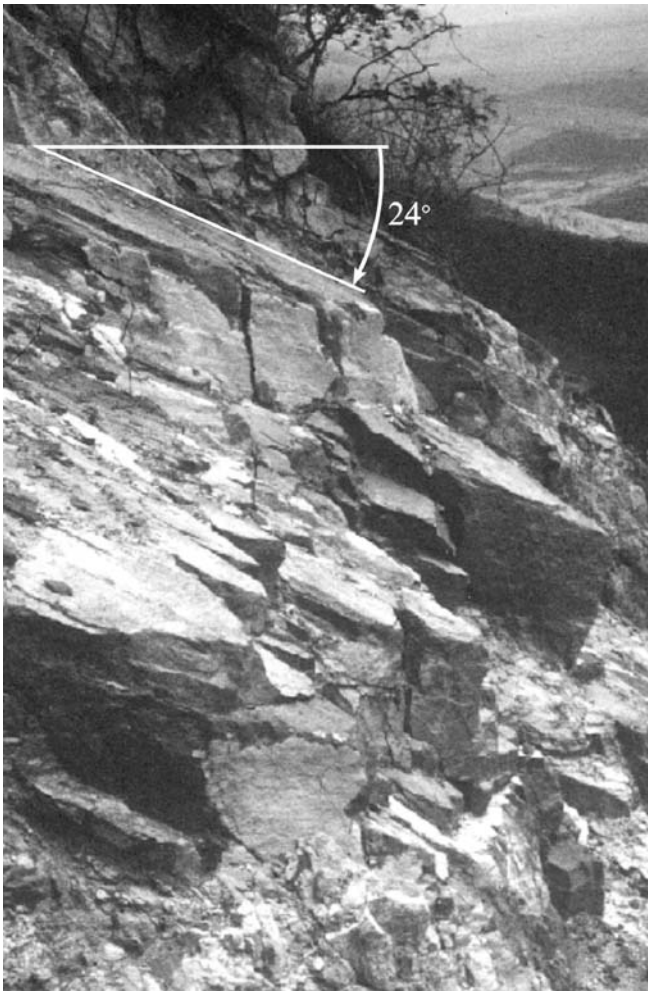
Fig. 11 Lava and tephra lithologies dipping south by as much as 24°. Viewing direction is towards the east. Photo location is indicated in Fig. 5a

drainage. Maintenance of such deep-seated water tables requires long, continuous rainfall periods (Iverson and Major 1987; van Asch et al. 1999).

Calculations by Iverson and Reid (1992) have shown that a uniform increase in pore pressure alone does not alter the effective stress state within a slope. Instead, instability results from pressure fluctuation, also noted by Harper (1975, p. 178): "Brief periods of intense rainfall generate a subsequent transient pressure rise in the rock mass, and this brief pressure wave may change a condition of stability in a rock slope to one of instability and movement." Such rainfall episodes preceded the Casita collapse on 30 October.

Pressure waves resulting from single rainfall events tend to attenuate before reaching the base of the landslide (Iverson and Major 1987). Harper (1975) reported an average time lag between rainfall and pressure rise of 1–3 days. The Casita collapse occurred approximately 12 h after a series of high-intensity rainfall event. This may indicate a high degree of fracturing leading to rapid infiltration or, alternatively, a high water table conveying

a fast pressure rise (Harper 1975). Surface flow drainage is not slope-parallel, but produces a curved flow field that directs seepage forces outwards from the slope (Iverson and Reid 1992). Such flow, which also leads to shear stress, is facilitated where low-conductivity layers are encountered (Reid and Iverson 1992), a condition provided by the clay-rich bedrock layer. At Casita this was increased by flank material dipping towards the south by as much as 24° (Fig. 11).

Discussion

At Casita, edifice-wide deformation and sector-collapse potential involving as much as 0.75 km^3 of material has been hypothesised (van Wyk de Vries et al. 2000). Deformation that may result in such a collapse in the future, however, has also generated instability on a smaller scale, setting the stage for the 1998 flank failure (Kerle and van Wyk de Vries 2001). Excessive precipitation is usually given as the trigger for the 1998 Casita lahar (Scott et al. 2003) because the flank collapse that led to the devastating flow occurred towards the end of a period of high rainfall associated with Hurricane Mitch. However, the absence of any large-scale failure following a comparable rainfall episode during Tropical Storm Alleta in 1982 suggests that precipitation is only one parameter governing such failures, or that more than just an isolated rainfall event must be considered. To this end we have investigated the contribution of other factors, in particular slope undercutting by gully migration, seismic activity and anthropogenic land cover changes, in generating a stability situation different from 1982.

Structural integrity of a flank can be compromised by erosional undercutting (Kelsey 1988; Corominas and Moya 1999). A stereoscopic analysis of aerial photographs has shown however, that principal gullies downstream from the failure site did not extend significantly in size and extent over a 42-year period. Similarly, an existing depression at the base of the flank showed no signs of change during that time. A survey of two gullies that were cleared of vegetation during the avalanche mirrored the morphological stability. No significant changes were measured during a period that saw 1,600 mm of rainfall.

Seismic activity is a key trigger of mass movements, capable of initiating thousands of shallow landslides over large areas (Keefer 1994), as well as large-scale edifice failure (McGuire 1996; Scott et al. 2001). Seismic data for the Casita-San Cristobal area contain significant noise from surface runoff and small debris flows generated by Mitch. This has masked the signal of the 30 October flank collapse, preventing a further constraining of the time of the event (W. Strauch, INETER, personal communication). However, the signal of an earthquake with trigger potential would likely have exceeded the noise. Because no seismic events were recorded at other stations, we discount a seismic trigger. However, Casita's edifice is bisected by tectonic and volcanic faults, and many
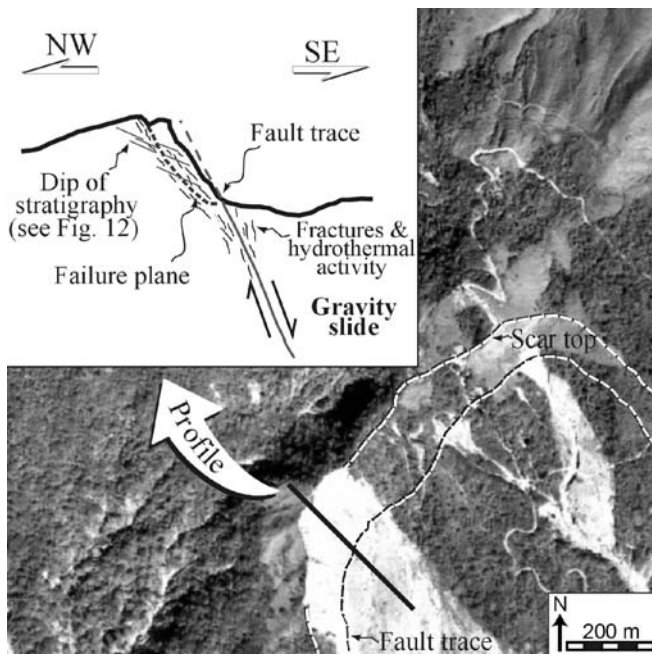
Fig. 12 Post-failure orthophoto, superimposed with the approximate location of the gravity slide boundary fault and the top of the scar. *Inset* shows a structural cross section of the failure cliff

earthquakes have occurred in its vicinity in the past. Damage reports for seismic events in 1938 and 1955 indicate a strong intensity amplification by the volcanic structures, as well as the ability of such events to open new surficial cracks and fissures. Given that several comparable earthquakes occurred between Alleta and Mitch, notably in 1983 and 1987 (magnitudes of 6.0 and 6.2, respectively), we can assume that those events had a cumulative destabilising effect on Casita's summit area. The consequences for the 1998 failure site could have been particularly severe, as the failure plane runs above the gravity slide-bounding fault (Fig. 12).

Landcover changes, in particular deforestation, have also been linked to slope instability in the past (DeRose et al. 1993), although they have more pronounced effects on surface layers (McKean et al. 1991). Although land use over the last century has changed markedly on Casita's flanks and the surrounding plains, no land cover changes were reported or observed in the vicinity of the failure site.

Conclusions

None of the factors discussed above appears to have been involved in triggering the 1998 collapse, suggesting that precipitation was indeed the responsible factor. However, it must be seen in the context of other parameters. We can identify several prerequisites for failure: (1) highly fractured material allowing deep and rapid infiltration, (2) less permeable material to impede drainage, (3) significant and continuous antecedent rain to build up a

perched water table with associated high pore pressure, and (4) episodic, high-intensity rainfall to establish recurrent pressure waves. Condition (1) was aided by edifice-deformation and gravity slide formation (with the boundary fault close to the failure site), seismic activity and local subsidence. Intense hydrothermal alteration, which is commonly strongest in the vicinity of dikes and open fractures (Reid et al. 2001), led to a clay-rich bedrock layer, satisfying prerequisite (2). More than 1,900 mm of rain fell in the months before Mitch. Corominas and Moya (1999) suggested that 2 weeks of very low rainfall are sufficient to cancel the effect of previous strong rain. Figure 10b shows that pre-Mitch rain was uninterrupted, meeting condition (3). Finally, condition (4) was met by strong, episodic rainfall during Mitch.

Conditions (1), (2), and (4) were probably satisfied during Tropical Storm Alleta as well. However, there was no significant antecedent rainfall. Note that, although nearly 1,600 mm of rain were recorded in Chinandega during the entire Mitch episode, 750 mm were sufficient to trigger the collapse. Nearly 1,500 mm during Alleta were not enough to build up the required deep-seated pore pressure. This picture conforms to a conclusion by Corominas and Moya (1999) that only shallow flows are generated in situations without antecedent rain, whereas strong precursory rain leads to deep-seated landslides (see also Iiritano et al. 1998).

The necessary coincidence of four failure conditions also explains why no sizeable flank failures occurred elsewhere on Casita during Mitch. Given (1) that the seasonal rainfall preceding the hurricane was average, (2) ongoing edifice deformation, and (3) remaining steep slopes along the headwalls of the gravity slide, a future rain event similar to Mitch or Alleta occurring towards the end of the rainy season can be expected to lead to further flank failures.

Risk is normally expressed as the product of hazard and vulnerability (Blaikie et al. 1994). Although anthropogenic activity has in the past been shown to influence slope stability (Alexander 1992; Wasowski 1998), there is no evidence for any such effects on the failure flank's structural integrity, i.e. the hazard. Conversely, vulnerability was generated when settlements were established on Casita's southern slope, on top of old lahar deposits, and greatly amplified by progressive northward deforestation. The reduced hydraulic roughness not only permitted a largely unimpeded flow, but also facilitated the bulking of the material that constituted most of the lahar when it destroyed the towns. Figure 13 summarises all factors influencing the hazard, trigger, and vulnerability.

The 1998 disaster demonstrates not only the severity of lahars resulting from comparatively small flank collapses, but also the difficulty in detecting the hazard. Despite extensive fieldwork, Hazlett (1977, p. 176) saw the lahar threat confined to the upper watershed and concluded: "...this favours continuation of present land use in the Casita watershed, and does not suggest to relocate towns and haciendas".
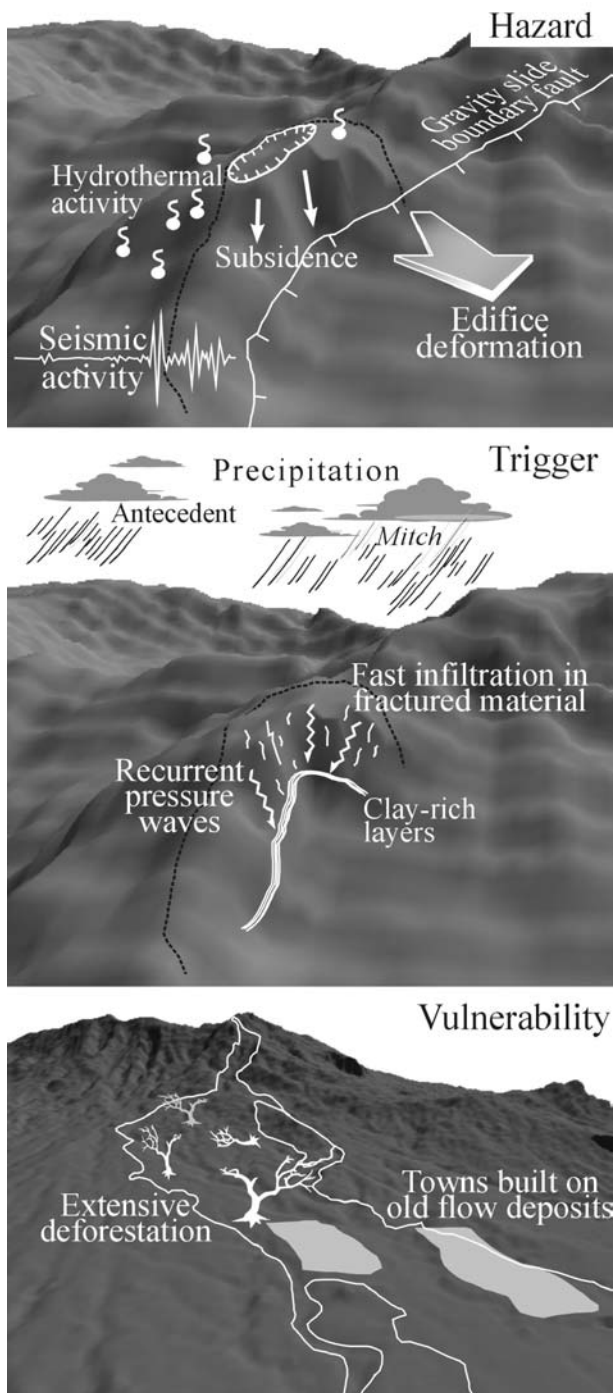
Fig. 13 Cartoon summarising factors that influenced the flank collapse hazard and trigger, and the vulnerability of towns on Casita's southern flank. *Dashed line* denotes collapse scar

References

Alexander D (1992) On the causes of landslides – human activities, perception, and natural processes. Environ Geol Water Sci 20:165–179

Barreto PE (1998) Testimonios relacionados con los ruidos y imagenes fatales segundos antes de la tragedia, llegada repentinamente desde del volcán Casitas a las comunidades Rolando Rodriguez y El Porvenir (in Spanish). Instituto Nicaragüense de Estudios Territoriales, Managua, Nicaragua, pp 1–9

Blaikie P, Cannon T, Davis I, Wisner B (1994) At risk: natural hazards, people's vulnerability, and disasters. Routledge, London, pp 1–284

Bolt BA, Hansen RA (1977) The upthrow of objects in earthquakes. Bull Seismol Soc Am 67:1415–1427

Borgia A, Delaney PT, Denlinger RP (2000) Spreading volcanoes. Annu Rev Earth Planet Sci 28:539–570

Bouchon M (1973) Effect of topography on surface motion. Bull Seismol Soc Am 63:615–632

Corominas J, Moya J (1999) Reconstructing recent landslide activity in relation to rainfall in the Llobregat River basin, Eastern Pyrenees, Spain. Geomorphology 30:79–93

Day SJ (1996) Hydrothermal pore fluid pressure and the stability of porous, permeable volcanoes. In: McGuire WJ, Jones AP, Neuberg J (eds) Volcano instability on the Earth and other planets. Geol Soc Spec Publ 110:77–93

DeRose RC, Trustrum NA, Blaschke PM (1993) Post-deforestation soil loss from steepland hillslopes in Taranaki, New-Zealand. Earth Surf Process Landforms 18:131–144

Dieterich JH (1988) Growth and persistence of Hawaiian volcanic rift zones. J Geophys Res (B Solid Earth) 93:4258–4270

Dietrich WE, Wilson CJ, Montgomery DR, McKean J (1993) Analysis of erosion thresholds, channel networks, and landscape morphology using a digital terrain model. J Geol 101:259–278

Elsworth D, Voight B (1996) Evaluation of volcano flank instability triggered by dyke intrusion. In: McGuire WJ, Jones AP, Neuberg J (eds) Volcano instability on the Earth and other planets. Geol Soc Spec Publ 110:45–53

European Forest Institute (2000) Country reports Nicaragua. Available at http://www.efi.fi/cis/english/creports/nicaragua.phtml

Ferraro R, Vicente G, Ba M, Gruber A, Scofield R, Li Q, Weldon R (1999) Satellite techniques yield insight into devastating rainfall from Hurricane Mitch. EOS 80:505–514

Geli L, Bard PY, Jullien B (1988) The effect of topography on earthquake ground motion – a review and new results. Bull Seismol Soc Am 78:42–63

Harper TR (1975) The transient groundwater pressure response to rainfall and the prediction of rock slope instability. Rock Mech Min Sci Geomech Abstr 12:175–179

Hazlett RW (1977) Geology and hazards of the San Cristobal volcanic complex, northwestern Nicaragua. MSc Thesis, Darthmouth College, Hanover, NH

Hazlett RW (1987) Geology of the San-Cristobal volcanic complex, Nicaragua. J Volcanol Geotherm Res 33:223–230

Hovius N, Stark CP, Tutton MA, Abbott LD (1998) Landslide-driven drainage network evolution in a pre-steady-state mountain belt: Finisterre Mountains, Papua New Guinea. Geology 26:1071–1074

Iiritano G, Versace P, Sirangelo B (1998) Real-time estimation of hazard for landslides triggered by rainfall. Environ Geol 35:175–183

INETER (1999) Las lluvias del Siglo in Nicaragua (in Spanish). Instituto Nicaragüense de Estudios Territoriales, Managua, Nicaragua, pp 1–159

Iverson RM, Major JJ (1987) Rainfall, groundwater-flow, and seasonal movement at Minor Creek landslide, northwestern California – physical interpretation of empirical relations. Bull Geol Soc Am 99:579–594

Iverson RM, Reid ME (1992) Gravity-driven groundwater flow and slope failure potential. 1: Elastic effective stress model. Water Resour Res 28:925–938

Keefer DK (1994) The importance of earthquake-induced landslides to long-term slope erosion and slope-failure hazards in seismically active regions. Geomorphology 10:265–284

Kelsey HM (1988) Formation of inner gorges. Catena 15:433–458

Kerle N (2002) Volume estimation of the 1998 flank collapse at Casita volcano, Nicaragua a comparison of photogrammetric and conventional techniques. Earth Surf Process Landforms 27:759–771

Kerle N, Oppenheimer C (2002) Satellite remote sensing as a tool in lahar disaster management. Disasters 26:140–160

Kerle N, van Wyk de Vries B (2001) The 1998 debris avalanche at Casita volcano, Nicaragua – investigation of structural deformation as the cause of slope instability using remote sensing. J Volcanol Geotherm Res 105:49–63

López DL, Williams SN (1993) Catastrophic volcanic collapse – relation to hydrothermal processes. Science 260:1794–1796

McGuire WJ (1996) Volcano instability: a review of contemporary themes. In: McGuire WJ, Jones AP, Neuberg J (eds) Volcano instability on the Earth and other planets. Geol Soc Spec Publ 110:1–24

McKean J, Buechel S, Gaydos L (1991) Remote sensing and landslide hazard assessment. Photogramm Eng Remote Sensing 57:1185–1193

Mejia-Navarro M, Wohl EE, Oaks SD (1994) Geological hazards, vulnerability, and risk assessment using GIS – model for Glenwood-Springs, Colorado. Geomorphology 10:331–354

Montgomery DR, Dietrich WE (1988) Where do channels begin? Nature 336:232–234

Montgomery DR, Dietrich WE (1989) Source areas, drainage density, and channel initiation. Water Resour Res 25:1907–1918

Morales A (1998) Informe del viaje al volcán Casita (in Spanish). Instituto Nicaragüense de Estudios Territoriales (INETER) internal report, Managua, Nicaragua, pp 1–2

Reid ME, Iverson RM (1992) Gravity-driven groundwater flow and slope failure potential. 2: Effects of slope morphology, material properties, and hydraulic heterogeneity. Water Resour Res 28:939–950

Reid ME, Sisson TW, Brien DL (2001) Volcano collapse promoted by hydrothermal alteration and edifice shape, Mount Rainier, Washington. Geology 29:779–782

Rojas W, Bungum H, Lindholm C (1993) A catalog of historical and recent earthquakes in Central America. A report under the project reduction of natural disasters in Central America. NORSAR, Norway

Sapper K (1913a) Die mittelamerikanischen Vulkane (in German). Petermanns Geogr Mitteilungen 59:173

Sapper K (1913b) Entwurf von Höhenschichten der mittleren Vukanregion Nikaraguas (in German). Petermanns Geogr Mitteilungen 59:310–311

Scott KM, Macías JL, Naranjo JA, Rodríguez S, McGeehin JP (2001) Catastrophic debris flows transformed from landslides in volcanic terrains: mobility, hazard assessment, and mitigation strategies. US Geol Surv Prof Pap 1630:1–71

Scott KM, Vallance JW, Kerle N, Macías JL, Strauch W, Devolí G (2003) Catastrophic, precipitation-triggered lahar at Casita volcano, Nicaragua Flow bulking and transformation. Earth Surf Process Landforms (in press)

Sheridan MF, Bonnard C, Carreño R, Siebe C, Strauch W, Navarro M, Calero JC, Trujilo NB (1999) 30 October 1998 rock fall/avalanche and breakout flow of Casita volcano, Nicaragua, triggered by Hurricane Mitch. Landslide News 12:2–4

Spudich P, Hellweg M, Lee WHK (1996) Directional topographic site response at Tarzana observed in aftershocks of the 1994 Northridge, California, earthquake: implications for mainshock motions. Bull Seismol Soc Am 86:S193–S208

van Asch TWJ, Buma J, van Beek LPH (1999) A view on some hydrological triggering systems in landslides. Geomorphology 30:25–32

van Wyk de Vries B, Merle O (1998) Extension induced by volcanic loading in regional strike-slip zones. Geology 26:983–986

van Wyk de Vries B, Kerle N, Petley DN (2000) Sector collapse forming at Casita volcano, Nicaragua. Geology 28:167–170

Vicente GA, Scofield RA, Menzel WP (1998) The operational GOES infrared rainfall estimation technique. Bull Am Meteorol Soc 79:1883–1898

von Seebach K (1892) Über Vulkane Centralamerikas. Aus den nachgelassenen Aufzeichnungen (in German). Dieterich, Göttingen

Wasowski J (1998) Understanding rainfall-landslide relationships in man-modified environments: a case-history from Caramanico Terme, Italy. Environ Geol 35:197–209